BIOTROPIA ISSN: 0215-6334 | e-ISSN: 1907-770X
The Southeast Asian Journal of Tropical Biology
Vol. 33 No. 3, 2026: 378 - 388
DOI: 10.11598/btb.2026.33.3.2588

Research Paper

Check for updates

HEPATOPROTECTIVE EFFECT OF *Physalis angulata* L. LEAF ETHANOL EXTRACT AGAINST BUSULFAN-INDUCED LIVER DAMAGE IN FEMALE RATS

Elsi Rahmadhani[1], Aryani Sismin Satyaningtijas[2*], Damiana Eka Ekastuti[2], Ronald Tarigan[2], I Ketut Mudite Adnyane[3], Kusdiantoro Mohamad[3], Wahono Esthi Prasetyaningtyas[3], and Yanti Sulistyana[1]

[1]Graduate Students of Veterinary Biomedical Science, School of Veterinary Medicine and Biomedical Sciences, IPB University, Bogor 16680, Indonesia

[2]Division of Physiology, School of Veterinary Medicine and Biomedical Sciences, IPB University, Bogor 16680, Indonesia

[3]Division of Anatomy, Histology and Embryology, School of Veterinary Medicine and Biomedical Sciences, IPB University, Bogor 16680, Indonesia

ARTICLE HIGLIGHTS

- Busulfan can damage the liver by triggering oxidative stress
- Physalis angulata leaves show natural liver protective effects
- Extract reduced oxidative damage in liver tissue
- Liver structure improved after extract treatment
- Early treatment provided stronger liver protection than delayed use

Article Information

Received : 19 September 2025
Revised : 15 December 2025
Accepted : 30 March 2026
Available Online : 23 July 2026

***Corresponding author, e-mail:**
aryanisa@apps.ipb.ac.id

ABSTRACT

Liver disease is the leading cause of death worldwide, with drug-induced hepatotoxicity being a major contributing factor. Busulfan, an anticancer drug used to treat chronic myeloid leukemia, is cytotoxic to proliferating cells and can induce liver injury. *Physalis angulata* L. (ground cherry) contains bioactive compounds with hepatoprotective properties. This study aimed to evaluate the protective effects of an ethanol extract of Phyasalis angulata L. (EEPA) leaves on Busulfan-induced liver damage in female Sprague–Dawley rats. Twenty-five rats were randomly divided into five groups: P1 (normal control), P2 (Busulfan 40 mg/kg, single dose), P3 (extract 300 mg/kg, days 1–28), P4 (Busulfan + extract, days 1–28), and P5 (Busulfan + extract, days 14–28). The parameters assessed were alanine aminotransferase (ALT), aspartate aminotransferase (AST), and malondialdehyde (MDA) levels in the liver, and liver histology. Data were analyzed using one-way analysis of variance (ANOVA), followed by a post hoc test. The results showed that *Physalis angulata* L. extract did not cause significant differences in serum ALT and AST levels, but significantly reduced MDA concentrations and improved liver histological architecture. Busulfan administration significantly decreased the hepatocyte count and increased Kupffer and inflammatory cells, fatty degeneration, and necrosis. Early administration of the extract (P4) produced more pronounced hepatoprotective effects compared to delayed administration (P5), as indicated by improved MDA and histological findings. These findings suggest that EEPA leaves exert hepatoprotective effects against Busulfan-induced liver injury in rats, likely through antioxidant activity, as evidenced by subsequent histological improvements, highlighting its potential as a natural hepatoprotective agent.

Keywords: Busulfan, hepatoprotective properties, liver histopathology, *Physalis angulata* L., rats

INTRODUCTION

Liver disease remains a significant global health challenge, ranking among the top ten leading causes of mortality worldwide (Devarbhavi *et al.* 2023). Various etiological factors contribute to liver dysfunction, including viral and fungal infections, excessive alcohol intake, exposure to toxic substances, and adverse drug reactions. Among these, drug-induced liver injury is a growing concern, particularly with the use of anticancer agents such as Busulfan. Busulfan (1,4-butanediol dimethanesulfonate) is a bifunctional alkylating agent with antineoplastic properties that is widely used in the treatment of chronic myeloid leukemia. It acts by forming DNA crosslinks that inhibit DNA replication and RNA transcription, ultimately inducing apoptosis in rapidly proliferating cells. Its cytotoxic effects primarily target rapidly dividing cells by forming covalent DNA cross-links, thereby inhibiting replication and promoting apoptosis (Qin *et al.* 2016). However, this cytotoxicity is not exclusive to malignant cells; normal hepatic cells, particularly hepatocytes and liver sinusoidal endothelial cells, are also vulnerable, which increases the risk of hepatotoxicity. Recent studies have identified Busulfan-induced oxidative stress, endothelial cell dysfunction, and inflammation as key mechanisms underlying hepatic injury (Balakrishnan *et al.* 2023; Hao *et al.* 2023; Ma *et al.* 2021).

The liver is the primary organ responsible for metabolic regulation, including the biotransformation of Busulfan. Although Busulfan does not directly generate reactive oxygen species (ROS) as metabolic byproducts, its cytotoxic effects and metabolic processing in the liver can disrupt redox homeostasis and trigger oxidative stress. This condition promotes excessive ROS production, which in turn induces lipid peroxidation in hepatocyte membranes. This peroxidation process generates toxic secondary products, such as malondialdehyde (MDA), a stable end-product widely recognized as a reliable biomarker of oxidative damage (Abarikwu *et al.* 2022).

Oxidative stress-induced liver injury often results in the leakage of intracellular enzymes, such as alanine aminotransferase (ALT) and aspartate aminotransferase (AST), into the bloodstream, making these enzymes reliable indicators of hepatocellular damage. Therefore, measuring the levels of these enzymes is vital to assess the extent of liver damage. Supplementation with exogenous antioxidants is essential for neutralizing excess ROS, inhibiting lipid peroxidation, and preserving the integrity of the liver cell membranes. Several studies have reported that natural antioxidants, particularly phenolic and flavonoid compounds derived from medicinal plants, are effective in lowering MDA levels and normalizing ALT and AST activities, thereby promoting liver recovery (Liao *et al.* 2024).

Physalis angulata L., a tropical plant commonly found along forest edges and in residential areas in Indonesia, has attracted attention for its hepatoprotective properties. These benefits are primarily attributed to the high content of flavonoids and phenolic compounds that act as potent antioxidants (Angela *et al.* 2023). Considering that numerous hepatoprotective agents originate from natural sources, *Physalis angulata* L. has been identified as a potential herbal candidate for liver protection (Melchart *et al.* 2017). Previous studies on similar hepatoprotective interventions had primarily used male rats; therefore, using female rats in the present study allows for evaluation of potential sex-related differences in liver response and provides complementary data. Therefore, the present study aimed to evaluate the effects of *Physalis angulata* on liver function by assessing serum ALT and AST activities, malondialdehyde (MDA) levels, and histopathological changes in rat liver tissues.

MATERIALS AND METHODS

Study Location

The study was conducted in the Laboratory Animal Management Unit at the School of Veterinary Medicine and Biomedicine (SKHB) of IPB University. The preparation of *Physalis angulata* and the analysis of samples were performed in the Physiology and Histology Laboratory of IPB University.

Experimental Animals and Study Design

A total of twenty-five female Sprague Dawley rats, aged 8 weeks and weighing 150 – 200 g, were obtained from the School of Veterinary and Biomedical Science, IPB University. This study was conducted following ethical guidelines and was approved by the Animal Ethics Commission of IPB University (certificate number 247/KEH/SKE/IX/2024). The study was conducted over 28 days using a Completely Randomized Design (CRD). P1 (normal control), P2 (Busulfan 40 mg/

kg, single dose), P3 (extract 300 mg/kg, days 1 – 28), P4 (Busulfan 40 mg/kg + extract, days 1 – 28), and P5 (Busulfan 40 mg/kg + extract, days 14 – 28).

Preparation of Phyasalis angulate Extract

The extraction of *Physalis angulata* leaves were extracted using the maceration method outlined by Angela *et al.* (2023). To prepare the extract, 70% ethanol was mixed with *Physalis angulata* leaf powder in a 5:1 ratio. The extract was prepared in three separate soaking periods. Each 24-hour soaking used a fresh portion of 70% ethanol, resulting in three consecutive extraction cycles. The macerated *Physalis angulata* leaf ethanol extract was evaporated using a rotary evaporator at 40 °C and 50 rpm, effectively removing the solvent to yield a concentrated extract of *Physalis angulata*. Subsequently, this extract was diluted to form a stock solution. This ratio was determined based on the standard preparation of a 10% (w/v) stock solution, where 20 g of extract was dissolved in 200 mL of aqueous solution.. Based on this stock solution, a dose of 300 mg/kg body weight corresponds to a concentration of 60 mg/mL. The dosage administered orally using a gastric tube to the rats was adjusted according to their body weights, given once daily throughout the duration of the study, following the designated group.

Preparation and Administration of Busulfan

The Busulfan dilution was prepared by weighing 0.24 g of solid Busulfan (0.5 g) and then adding concentrated dimethyl sulfoxide (DMSO) (99.5%). The mixture was then homogenized. Next, 4.5 mL of warmed phosphate-buffered saline (PBS) at 37 °C was added to the Busulfan-DMSO solution. The solution was further homogenized using a vortex mixer, filtered through a 0.22 µm syringe filter, and transferred into a microcentrifuge tube. The Busulfan concentration in the solution was 48 mg/ml. Busulfan was administered to the rats via intraperitoneal injection at a single dose of 40 mg/kg.

Sample Collection

At the end of the experimental period, the rats were euthanized using a high dose of ketamine and xylazine to ensure humane termination. Liver tissues were then carefully excised for biochemical and histological analysis. All procedures were performed following ethical guidelines to minimize animal distress.

Assessment of Liver Function (ALT and AST Levels)

Blood samples was collected via intracardiac puncture under anesthesia at the end of the study. This route was chosen as a terminal procedure to obtain an adequate volume of high-quality blood necessary for multiple biochemical analyses, while minimizing stress and discomfort to the animals. The blood samples were placed in vacutainer tubes (One Med®) and subsequently centrifuged at 2,500 rpm for 15 minutes to separate the serum. ALT and AST activities were measured in the serum using the UV kinetic method, following the manufacturer's instructions provided in the ReiGed kit (ALT: GPT-11100; AST: GOT-11100), where ΔAbs/min was multiplied by 1768 and 1746, respectively to obtain the enzyme activity in U/L. For the assay, 1,000 µL of the working reagent was added to a cuvette and incubated at 37°C for 1 minute. Next, 100 µL of serum sample was added. The activities of ALT and AST were then measured using a UV-VIS spectrophotometer at a wavelength of 340 nm. Absorbance was measured at 1 minute and 3 minutes. Absorbance was calculated using the following formula:

$$\textbf{ALT (U/L)} = \Delta\textbf{Abs/min} \times \textbf{1768}$$

$$\textbf{AST (U/L)} = \Delta\textbf{Abs/min} \times \textbf{1746}$$

Measurement of Liver Malondialdehyde (MDA)

Malondialdehyde concentration were measured using the Thiobarbituric Acid Reactive Substances (TBARS) method described by Alfarisi *et al.* (2022). The rats were humanely euthanized under deep anesthesia using a high dose of ketamine and xylazine, following standard ethical guidelines to minimize animal suffering. After euthanasia, approximately 0.5 g of liver tissue was weighed and finely chopped. The tissue was then homogenized in 5 mL of phosphate-buffered saline (PBS). The homogenate was transferred into a centrifuge tube and centrifuged at 3,500 rpm for 10 minutes in a pre-cooled centrifuge at 4 °C. All homogenization and handling steps were performed on ice to maintain cold conditions, minimizing anzymatic activity and lipid peroxidation, thereby preserving sample integrity for accurate MDA measurement. The resulting supernatant was collected in chilled Eppendorf tubes.

One mL supernatant was transferred into a test tube, followed by the addition of 4 mL of a cold reagent mixture consisting of 0.25 N

HCl containing 15% trichloroacetic acid (TCA), 0.38% thiobarbituric acid (TBA), and 0.5% butylated hydroxytoluene (BHT). The mixture was then incubated in an oven at 80 °C for 1 hour. After incubation, the tubes were cooled in a water bath with running tap water for 10 minutes and then centrifuged at 3,500 rpm for 10 minutes at 4 °C. The absorbance of the supernatant was measured at 532 nm using a UV-Vis spectrophotometer. A standard curve was prepared using 1,1,3,3-tetraethoxypropane (TEP) at concentrations of 0, 0.05, 0.025, 0.1, and 0.2 mMol. MDA levels were determined using linear regression analysis based on the TEP standard curve. This chain reaction ultimately results in the production of MDA, which can be quantitatively measured in tissues or serum using methods such as the thiobarbituric acid reactive substance (TBARS) assay (Mas-Bargues *et al.* 2021).

Histolopathological Examination (Sample Preparation)

The rats were euthanized at the end of this study and dissected to take the livers for examined any visible abnormalities. A representative section from one liver lobe was selected for each treatment group. This approach ensured consistent and comparable evaluation of hepatocellular structure while minimizing tissue use. Liver tissue samples were collected and fixed in 4% paraformaldehyde (PFA) for seven days. The fixed samples were subjected to standard histological processing, which included dehydration, clearing, embedding in paraffin, sectioning, staining, and mounting according to the protocol described by Alfarisi *et al.* (2022). Tissue sections were cut at a thickness of 5 μm and stained with Hematoxylin and Eosin (HE).

Histological Analysis (Analytical Method)

Microscopic observation of the liver tissue was conducted using a quantitative descriptive approach, focusing on the areas surrounding the central vein across five different fields of view for each sample. The images were captured and quantified at 400× magnification. Tissue observations and image acquisition were performed using a CX31 light microscope (Olympus) equipped with a CCD10-USB camera. Quantitative analysis was performed using ImageJ software version 1.53q (FIJI), allowing for precise measurement and evaluation of histological parameters. The number of hepatocytes, Kupffer cells, inflammatory cells, fat-laden cells, and necrotic cells was counted in each field, and the mean values were calculated to obtain representative data for each treatment group.

Cell Identification Criteria

Identification of necrotic and inflammatory cells was performed based on established histomorphological characteristics. Necrotic hepatocytes were identified by the presence of lost or faintly stained nuclei indicative of karyolysis, intense cytoplasmic eosinophilia, cellular swelling or fragmentation, and disruption of the normal sinusoidal architecture. Areas of necrosis frequently appeared as confluent patches or regions of coagulative necrosis.

Inflammatory leukocytes were characterized as small, round cells with dense basophilic nuclei. Neutrophils were distinguished by their multilobed nuclei and pale granular cytoplasm, whereas lymphocytes appeared smaller with dark, condensed nuclei. Macrophages were identified as larger cells with abundant, often vacuolated cytoplasm.

Data Analysis

The data were processed using Microsoft Excel to calculate the mean and standard deviation. Before further analysis, the data were tested for normality and homogeneity to ensure that the assumptions for the ANOVA were met. Statistical analysis was performed using SPSS software version 23 (IBM Corp., Armonk, NY, USA). One-way ANOVA was conducted at the 5% significance level, and if a significant difference was found, a post-hoc Duncan's multiple range test was applied to identify differences between groups.

RESULTS AND DISCUSSION

Liver Functional Assessments

Alanine aminotransferase (ALT) and aspartate aminotransferase (AST) are important biochemical markers used to evaluate liver health and function. ALT is a liver-specific enzyme found in the cytoplasm of liver cells, and its levels increase in the bloodstream when the hepatocyte membranes are damaged. In contrast, AST is present in both the cytoplasm and mitochondria of cells, and typically increases in cases of more severe or systemic liver damage (Yaman *et al.* 2024). The results of this study indicated no statistically significant differences in ALT ($P = 0.762$) or AST

(P = 0.533) levels between the treatment groups (Fig. 1A & 1B). This suggested that the treatment did not cause any significant hepatotoxic effects.

The highest ALT level was observed in group P2, with an average value approaching 60 IU/L (Fig. 1A), which is slightly above the normal range for Sprague Dawley rats (typically 30 – 50 IU/L). This finding indicates potential liver injury induced by Busulfan injection. Although the difference between the control (P1) and treatment groups was not statistically significant, this trend is supported by other parameters. Specifically, group P2 also showed elevated MDA levels and histopathological alterations, indicating mild hepatocellular stress. Therefore, the ALT results are interpreted in conjunction with complementary biochemical and histological findings rather than in isolation.

The lowest ALT level was recorded in group P3, remaining below 50 IU/L and comparable to group P1. This suggests that the administration of *Physalis angulata* leaf ethanol extract did not cause hepatocellular damage, which could trigger the release of ALT into the circulation. Furthermore, group P4 exhibited lower ALT levels than group P5, which may be attributed to the longer duration of administration of *Physalis angulata* ethanol extract.

The highest AST level was also found in group P2, which approached 150 IU/L (Fig. 1B). The increase in AST in this group reflects the hepatic response to exposure to toxic agents, such as Busulfan. Busulfan possesses hepatotoxic potential by inducing oxidative stress, mitochondrial dysfunction, and activation of apoptotic pathways in hepatocytes (Hao *et al.* 2023). The elevated AST activity in this group suggested the presence of subclinical damage or mild metabolic stress in liver cells, although the difference was not statistically significant. The AST level in group P3 was slightly lower than that in group P2 (145 IU/L), indicating that administration of *Physalis angulata* extract alone was not sufficient to optimally reduce AST activity.

Physalis angulata contains active compounds, such as withanolides, flavonoids, and physalins, which have been reported to exert antioxidant, anti-inflammatory, and hepatoprotective activities. However, the effectiveness of its protective effects against liver injury is strongly influenced by dosage, duration of administration, and degree of oxidative stress (Wiraswati *et al.* 2024). Groups P4 and P5 showed a trend of reduced AST levels compared with groups P2 and P3, indicating that *Physalis angulata* administration concomitant with Busulfan provided hepatoprotective effects against liver damage.

The higher AST level in group P4 may be related to the initiation of *Physalis angulata* extract during the acute phase of Busulfan-induced hepatic injury. At this stage, hepatocytes experience intense necro-inflammatory stress, which may limit the extract's hepatoprotective capacity. In group P5, the delayed administration (day 14) coincided with the early recovery phase, allowing the extract to act more effectively and resulting in lower AST levels. AST is an enzyme present in the liver and other tissues, including muscle and kidney. In this study, AST levels in all groups remained within the normal range, indicating that there was no significant tissue damage. The normal range for ALT is 30-50 IU/L, whereas that for AST is 60-150 IU/L (Wozniak *et al.* 2021).

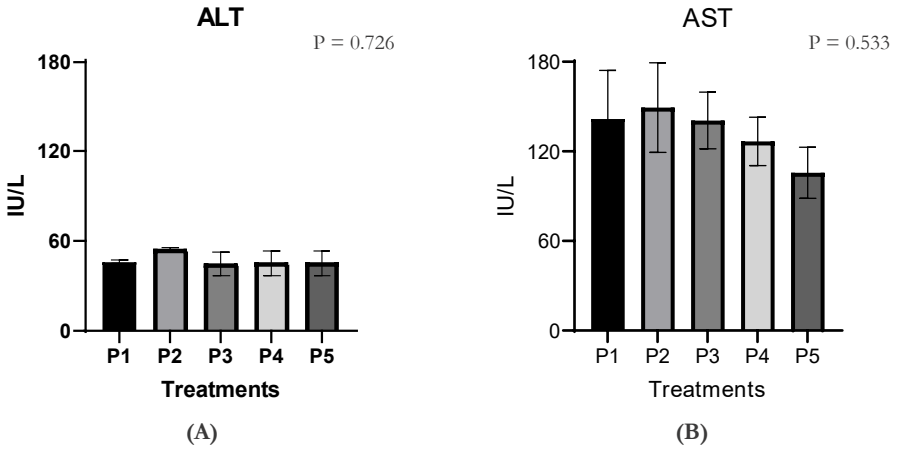

Figure 1 Effect of treatment on ALT and AST levels

Notes: P1 = normal control; P2 = Busulfan 40 mg/kg BW, single dose; P3 = extract 300 mg/kg BW, days 1 –28; P4 = Busulfan 40 mg/kg BW + extract, days 1 – 28; and P5 = Busulfan 40 mg/kg BW + extract, days 14 – 28). The vertical line (bar) is the standard error.

Malondialdehide (MDA) Levels

Malondialdehyde is the final product of lipid peroxidation, which damages cell membranes through reactions between reactive oxygen species (ROS) and unsaturated fatty acids present in phospholipid membranes. MDA is commonly used as a biomarker for oxidative stress, especially in conditions involving cell injury, including liver damage. Lipid peroxidation begins when hydroxyl radicals (•OH) attack the double bonds in unsaturated fatty acids, leading to the formation of unstable lipid peroxides.

Malondialdehyde levels in rat liver tissue, as illustrated in Figure 2, were significantly different among the treatment groups ($P < 0.05$).

Group P1 had the lowest MDA level at 0.21 nmol/g, whereas the group treated with Busulfan (P2) exhibited a notable increase in MDA levels to 0.34 nmol/g. This suggests that Busulfan may induce liver damage through mechanisms involving inflammatory responses, oxidative stress, metabolism, and signaling pathways associated with liver injury.

Busulfan significantly enhances the expression of various genes and proteins associated with inflammation and hepatocellular injury (Hao *et al.* 2023). It triggers the upregulation of proinflammatory cytokines, including interferon-gamma (IFN-γ), interleukin-6 (IL-6) and its receptor (IL-6R), interleukin-22 receptor (IL-22R), transforming growth factor-beta (TGF-β), and tumor necrosis factor-alpha (TNF-α). The activation of these cytokines stimulates both systemic and local inflammatory responses, engaging the Janus kinase (JAK) and Signal Transducer and Activator of Transcription 3 (STAT3) signaling pathways, particularly within hepatocytes. Chronic activation of STAT3 not only promotes abnormal cell proliferation but also increases the expression of Tribbles Pseudokinase 3 (TRIB3), which serves as a mediator of cell stress and apoptosis. TRIB3 functions by inhibiting cell survival pathways such as the Phosphoinositide 3-Kinase (PI3K) pathway, thereby increasing the susceptibility of hepatocytes to cell death (Hao *et al.* 2023).

The increase in MDA levels observed in group P2 was linked to elevated ALT and AST levels compared to those in group P1 ($P > 0.05$). Conversely, group P4 showed a notable reduction in MDA levels compared with group P2, reaching approximately 0.28 nmol/g. This finding suggests that *Physalis angulata* may have a protective effect against oxidative stress induced by Busulfan. *Physalis angulata* is rich in bioactive compounds such as flavonoids and polyphenols, which are known for their ability to scavenge free radicals, inhibit lipid peroxidation, and bolster the body's endogenous antioxidant defense system. Research conducted by Tampie *et al.* (2023) reported that the total flavonoid content of *Physalis angulata* leaves was 2.29% (w/w). The antioxidant activity of *Physalis angulata* leaf extract is thought to aid in preventing the formation of free radicals, thereby reducing the generation of radical unsaturated fats.

The MDA level in group P3 was higher than that in group P1, suggesting that although *Physalis angulata* possesses antioxidant properties, its administration to healthy animals without stressors may induce an adaptive biological response. Furthermore, group P4 received *Physalis angulata* extract immediately after Busulfan exposure, which allowed early suppression of reactive oxygen species and limited lipid peroxidation, resulting in lower MDA level. In contrast, the delayed administration in P5 allowed oxidative damage to occur before intervention, leading to higher MDA level.

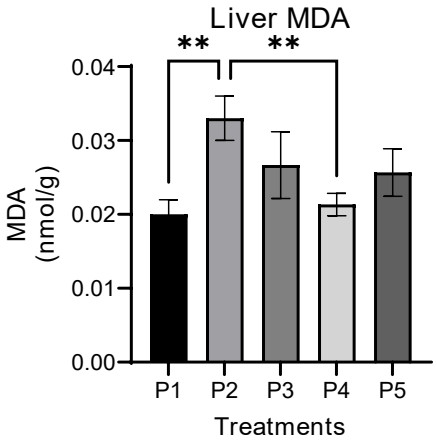

Figure 2 Effects of treatment on liver MDA
Notes: P1 = normal control; P2 = Busulfan 40 mg/kg BW, single dose; P3 = extract 300 mg/kg BW, days 1 – 28; P4 = Busulfan + extract, days 1 – 28; and P5 = Busulfan + extract, days 14 – 28. The vertical line (bar) represents the standard error.

Histological Examination

Photomicrographs of the rat livers are shown in Figure 3. Histological analysis revealed that Busulfan treatment significantly altered the microscopic structure of rat liver. The control group (Fig. 3A) displayed normal liver architecture, characterized by a well-organized arrangement of hepatocytes surrounding a central vein, with sinusoids that were narrow and relatively uniform in size. The hepatocytes exhibited one or two round nuclei and displayed distinct chromatin. In contrast, the Busulfan-treated group (Fig. 3B) showed pronounced degenerative changes in liver architecture. The hepatocytes appeared disorganized and exhibited signs of cytoplasmic vacuolization, necrosis, and infiltration by inflammatory cells.

The *Physalis angulata* group displayed a nearly normal liver structure (Fig. 3C), indicating that a single dose of *Physalis angulata* does not result in liver toxicity. In contrast, liver microphotographs from group P4 showed an improved liver tissue structure, characterized by more organized hepatocytes. However, signs of damage, including necrosis and inflammatory infiltration, were still evident (Fig. 3D). This suggests that the early administration of *Physalis angulata* may prevent the hepatotoxic effects of Busulfan. Group P4 showed reduced hepatocellular necrosis, sinusoidal congestion, and inflammatory infiltration; although the scores remained above normal, they were lower than in P5. The percentages of necrotic cells, Kupffer cells, leukocytes, and fat cells were calculated as the proportions of each cell type within the total counted area (Table 1).

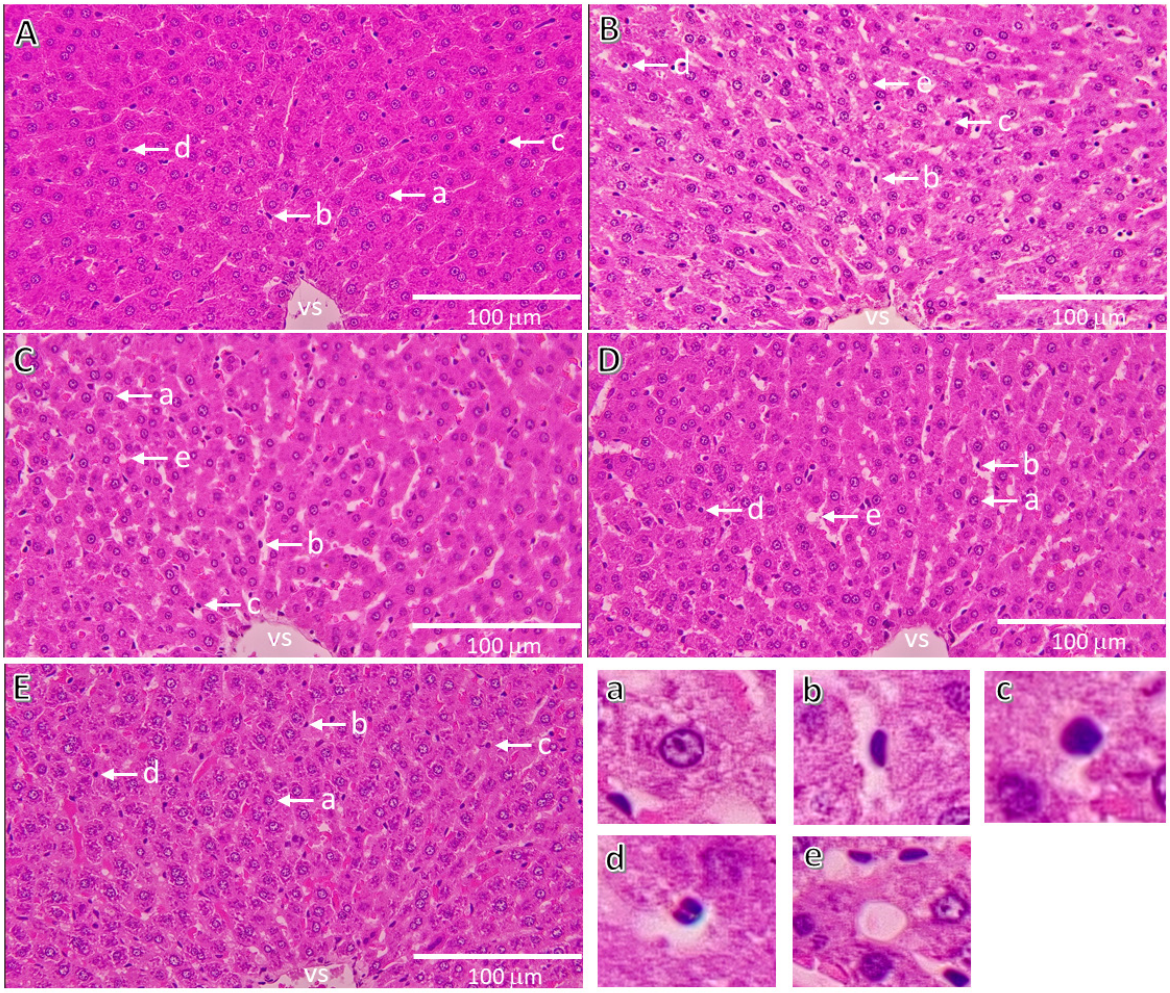

Figure 3 Photomicrograph of rat livers stained with Hematoxylin and Eosin

Notes: Scale bar = 100 µm. P1 = normal control; P2 = Busulfan 40 mg/kg, single dose; P3 (extract 300 mg/kg, days 1 – 28; P4 (Busulfan + extract, days 1 – 28; and P5 = Busulfan + extract, days 14 – 28. Vs = central vein; a = normal hepatocytes; b = Kupffer cells; c = necrotic cells; d = inflammatory cells; e = fatty degeneration.

Table 1 The percentage each cell type within the total counted area

Experimental Groups	% Nekrosis	% Kupffer	% Leukosit	% Fat cells
P1	0.81	12.12	15.94	0.37
P2	3.21	27.91	35.31	1.91
P3	2.65	21.04	25.71	0.49
P4	2.50	18.75	24.63	0.95
P5	3.01	15.90	21.02	1.17

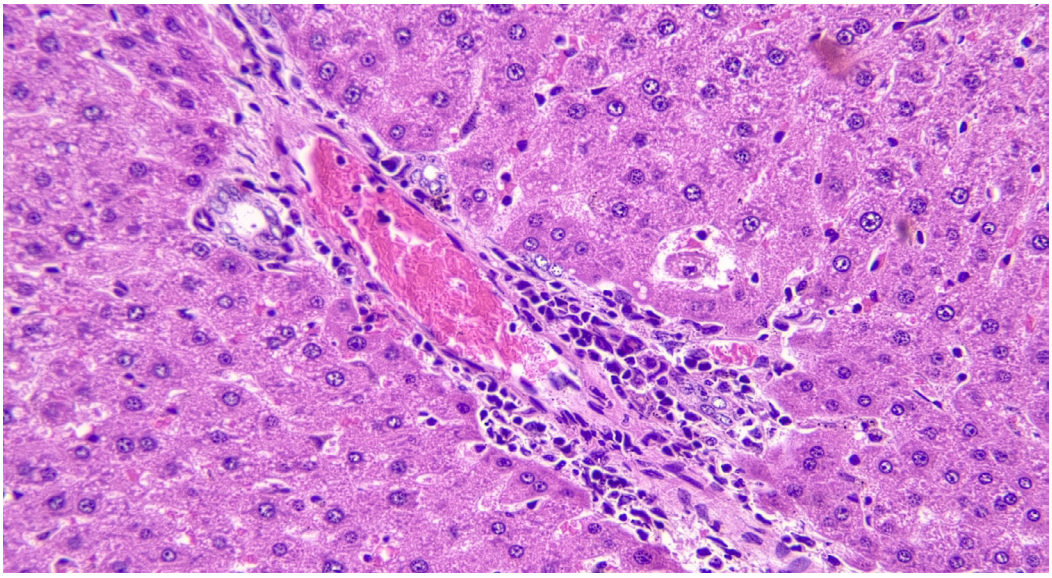

Figure 4 Representative histopathological image showing inflammatory cell infiltration in liver tissue

Notes: Hematoxylin–eosin (H&E) staining demonstrates focal inflammatory cell infiltration (arrow) predominantly localized in the portal area and extending into the surrounding hepatic parenchyma. Although the extent of infiltration is limited, the presence of clustered inflammatory cells indicates an inflammatory response within the liver tissue. Hepatocytes surrounding the infiltrated area appear relatively preserved. Original magnification: ×400.

The percentage of necrotic areas ranged from 0.81% to 3.21%, with P1 showing the lowest necrosis (0.81%) and P2 the highest (3.21%). Overall, all groups exhibited necrosis levels below 5%, indicating minimal hepatocellular damage across treatments. The narrow range among groups suggests that the experimental interventions did not induce substantial cell death or widespread necrotic lesions in the liver. Kupffer cell percentages varied more distinctly, ranging from 12.12% to 27.91%. The highest Kupffer cell proliferation occurred in P2 (27.91%), suggesting enhanced macrophage activation and a mild inflammatory response in this group, as shown in Figure 4. In contrast, P1 exhibited the lowest Kupffer cell percentage (12.12%). The moderate increase in Kupffer cells in P2 and P3 may reflect the liver's innate immune response to potential tissue injury or oxidative stress.

Leukocyte infiltration followed a similar pattern, with values between 15.94% and 35.31%. The most pronounced infiltration was again observed in P2 (35.31%), indicating a greater inflammatory reaction in this group. Meanwhile, P1 showed the lowest leukocyte percentage (15.94%). These findings align with the Kupffer cell profile, supporting the interpretation that P2 experienced the strongest inflammatory response among the groups, while P1 retained near-normal histological features. The percentage of fat cells was relatively low across all groups (0.37 – 1.91%). P2 showed the highest fat accumulation (1.91%), while P1 demonstrated the least (0.37%). Overall, fat deposition remained minimal, suggesting no significant steatosis. The slight increase observed in P2 and P5 may indicate early-stage lipid accumulation but remains within the range of mild hepatic alteration.

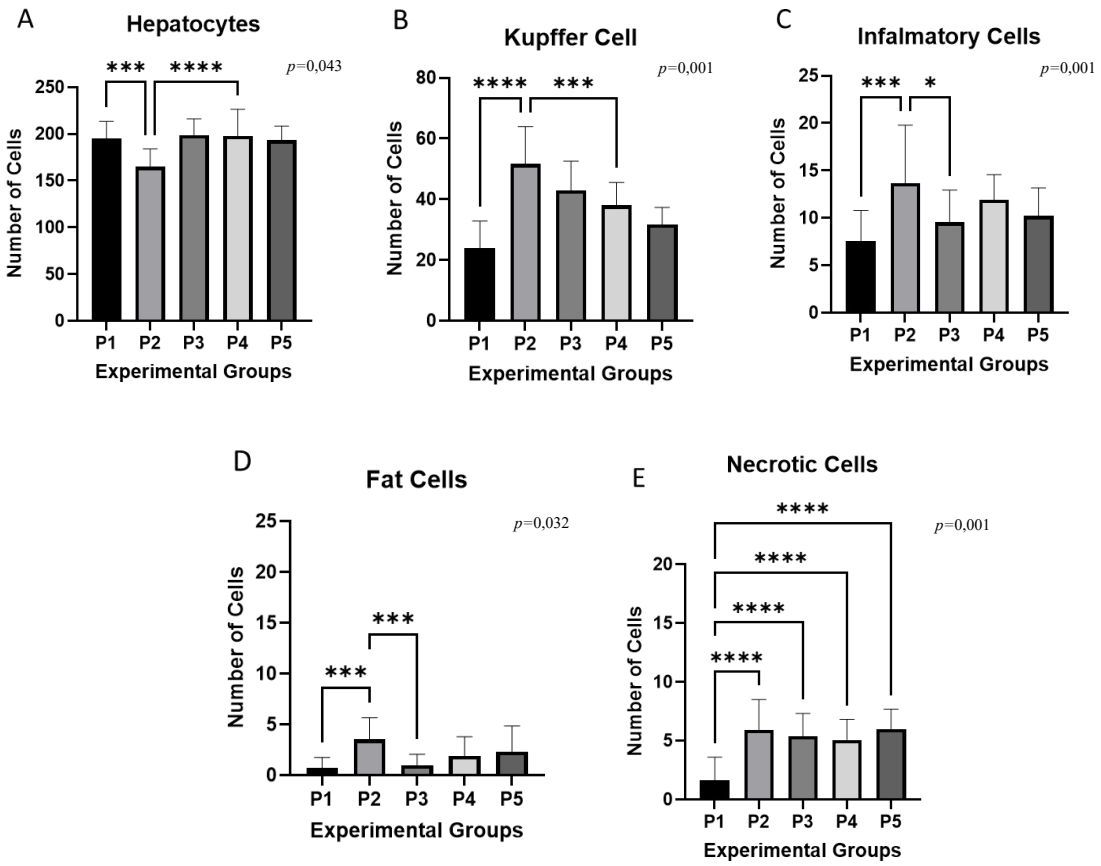

Figure 5 Quantitative effect of treatment on the histology of liver organs

Notes: A = Total hepatocytes; B = Kupffer cells; C = Inflammatory cells; D = Fat cells; E = Necrotic cells. P1 = normal control; P2 = Busulfan 40 mg/kg, single dose; P3 = extract 300 mg/kg, days 1 – 28; P4 (Busulfan + extract, days 1 – 28; and P5 Busulfan + extract, days 14 – 28. The vertical line (bar) represents the standard error. The asterisk indicates the level of significance of the difference between groups (* P < 0.05; *** P < 0.001; **** P < 0.0001).

All the groups showed significant changes in the mean total number of hepatocytes (Fig. 5A). Group P2 exhibited the lowest value compared with P1, which is likely attributable to Busulfan-induced liver damage. Velden *et al.* (2018) reported that Busulfan promotes the release of growth factor-β super-activin-A, triggering a pro-inflammatory response that contributes to hepatocyte injury. This process leads to the depletion of hepatic glutathione by Busulfan, which in turn exacerbates oxidative stress and elevates pro-inflammatory cytokines, such as TNF-α, thereby inducing hepatotoxicity.

In contrast, the groups treated with *Physalis angulata* extract showed no difference (P > 0.05) in the total hepatocyte counts compared to P1. This finding suggests that *Physalis angulata* may stimulate hepatocyte regeneration or exert protective effects. *Physalis angulata* leaves contain several bioactive compounds, including myricetin-type physalins and flavonoids. Myricetin has been reported to regulate ROS, suppress NF-κB transcriptional activity, and reduce IL-1β and TNF-α (Wang *et al.* 2019). Furthermore, physalins B, D, F, and G exhibit anti-inflammatory properties by inhibiting NF-κB–mediated signaling and consequently reducing IL-1β and TNF-α (Meira *et al.* 2022).

Group P2 exhibited the highest number of Kupffer cells, indicating pronounced immune activation, likely triggered by liver injury or inflammation (Fig 5B). Conversely, the group treated with *Physalis angulata* extract showed a reduced number of these cells. Kupffer cells are specialized liver-resident macrophages that play key roles in maintaining hepatic immune surveillance and homeostasis. Under normal physiological conditions, they act as primary defense mechanisms against microbial invasion. However, in response to pathological stimuli, these cells are activated and contribute to the inflammatory response. Owing to their distinctive metabolic profile and functional roles, Kupffer cells are considered promising targets for therapeutic interventions in liver-related inflammatory conditions, infections, and malignancies (Zhao *et al.* 2025).

Inflammatory cell accumulation was observed in all the treatment groups and showed significant changes (Fig. 5C). Group P2 exhibited the highest number of inflammatory cells, indicating severe hepatic inflammation. Group P3, on the other hand, demonstrated a potential protective effect, as the number of inflammatory cells was comparable to that of P1. Histopathological analysis showed that inflammatory cell infiltration in P4 was higher than in P5. This may reflect an active immune response during the early phase, which is part of tissue repair and regeneration, whereas P5, with delayed extract administration, showed less inflammatory infiltration but more extensive hepatocellular necrosis. Inflammation is a physiological response of the body to tissue injury, and is characterized by the recruitment of defense cells to limit further damage and promote tissue repair.

Busulfan damages sinusoidal endothelial cells, leading to the release of damage-associated molecular patterns (DAMPs) such as adenosine triphosphate (ATP) and high-mobility group box 1 (HMGB1). These signals activate caspase-1, resulting in the enhanced release of IL-1β and IL-18, which subsequently stimulate neutrophil and macrophage infiltration, thereby promoting inflammation (Qiao *et al.* 2015). *Physalis angulata* contains bioactive compounds, such as physalin D, which has been reported to attenuate hepatic fibrosis by inhibiting the transforming growth factor-β (TGF-β) and Yes-associated protein (YAP) signaling pathways (Xiang *et al.* 2020). Physalin D also effectively suppressed NF-κB receptor activation (Ding *et al.* 2020), contributing to its anti-inflammatory effects.

As shown in Figure 5D, fatty degeneration was present in the liver tissues across all treatment groups, with statistically significant differences ($P < 0.05$). Group P2 exhibited the most severe fatty changes, indicating substantial hepatic injury. In contrast, Group P3 demonstrated minimal fat accumulation, closely resembling the control group (P1), suggesting a protective effect of *Physalis angulata* administration. Fatty degeneration is marked by the formation of cytoplasmic vacuoles of varying sizes within the hepatocytes. This condition often results from disturbances in lipid metabolism, such as mitochondrial dysfunction or hypoxic conditions, which impair fatty acid oxidation and lead to lipid accumulation within the liver cells (Sijid *et al.* 2020).

As shown in Figure 5E, all treatment groups exhibited significant differences in the number of necrotic cells within liver tissue ($P < 0.05$). The highest necrotic cell count was observed in P2, reflecting the most extensive liver damage. Conversely, Groups P3, P4, and P5 showed reduced levels of necrosis, suggesting a protective effect of *Physalis angulata* L. extract. Busulfan is known to induce excessive generation of reactive oxygen species (ROS), which contributes to hepatocellular injury. The resulting oxidative stress damages hepatocytes and activates Kupffer cells, initiating fibrogenesis through the secretion of inflammatory cytokines and platelet-derived growth factors (Komolkriengkrai *et al.* 2019).

Prolonged liver injury stimulates hepatic stellate cells (HSCs) to transdifferentiate into myofibroblast-like cells, which secrete extracellular matrix (ECM). The accumulation of ECM can compromise vascular function and promote vascular shunting in both the portal and systemic circulation, thereby impairing the exchange of nutrients and oxygen between hepatocytes and sinusoidal blood. This disruption may result in hepatocyte apoptosis and further loss of liver function (Wu *et al.* 2016).

Histological profiles revealed that hepatocellular damage occurred in group P2 (Busulfan-only control), as evidenced by a reduction in total hepatocytes, an increase in Kupffer cells and inflammatory cells, and the presence of fatty degeneration and necrotic cells compared to group P1. Groups P4 and P5 demonstrated protective effects by restoring the number of hepatocytes and Kupffer cells to levels close to those of P1; however, they were unable to reduce inflammatory cell infiltration, fatty degeneration, and hepatocellular necrosis.

CONCLUSION

Physalis angulata L. extract did not cause significant differences in ALT and AST levels but significantly reduced MDA concentrations and improved liver histological architecture. Early administration of the extract (from day 1) demonstrated stronger hepatoprotective effects than delayed administration (from day 14 onwards), as shown by lower MDA levels and improved liver histological structure.

REFERENCES

Alfarisi H, Wresdiyati T, Sadiah S, Juliandi B. 2022. Nanoextract of Acalypha hispida leaves increases antioxidant defense and suppresses microstructure damage in liver and kidney of diabetic rats. J Appl Pharm Sci 12(10):99–108. DOI:10.7324/JAPS.2022.121010

Angela BT, Astuti DR, Adnyane IKM, Satyaningtijas AS. 2023. Ciplukan leaf extract (*Physalis angulata* L.) can potentially improve kidney function. Acta Vet Indones 11(1):9–16. DOI:10.29244/avi.11.1.9-16

Balakrishnan B, Illangeswaran RSS, Rajamani BM, Arunachalam AK, Pai AA, Mohanan E, …, Balasubramanian P. 2023. Metformin pre-treatment ameliorates busulfan-induced liver endothelial toxicity during hematopoietic stem cell transplantation. PLoS One 18(10):e0293311. DOI: 10.1371/journal.pone.0293311

Devarbhavi H, Asrani SK, Arab JP, Nartey YA, Pose E, Kamath PS. 2023. Global burden of liver disease: 2023 update. J Hepatol 79(2):516–537. DOI:10.1016/j.jhep.2023.03.017

Ding N, Lu Y, Cui H, Ma Q, Qiu D, Wei X, …, Cao N. 2020. Physalin D inhibits RANKL-induced osteoclastogenesis and bone loss by regulating calcium signaling. BMB Rep 53(3):154–159. DOI:10.5483/BMBREP.2020.53.3.147

Gęgotek A, Skrzydlewska E. 2019. Biological effects of protein modification by lipid peroxidation products. Chem Phys Lipids 221(2):46–52. DOI:10.1016/j.chemphyslip.2019.03.011

Hao Y, Fang H, Yan X, Shen W, Liu J, Han P, …, Feng Y. 2023. Alginate oligosaccharides repair liver injury by improving anti-inflammatory capacity in a busulfan-induced mouse model. Int J Mol Sci 24(4). DOI:10.3390/ijms24043097

Kalas MA, Chavez L, Leon M, Taweesedt PT, Surani S. 2021. Abnormal liver enzymes: A review by clinicians. World J Hepatol 13(11):1688–1698. DOI:10.4254/wjh.v13.i11.1688

Komolkriengkrai M, Nopparat J, Vongvatcharanon U, Anupunpisit V, Khimmaktong W. 2019. Effects of glabridin on collagen deposition in the liver and amelioration of hepatocyte destruction in diabetic rats. Exp Ther Med 17(6):1164–1174. DOI:10.3892/etm.2019.7664

Ma X, Yuan J, Liu X, Xu J, Han J, Wang X, Zhao L. 2023. Busulfan-induced hepatic sinusoidal endothelial cell injury: The modulatory role of pirfenidone for therapeutic purposes. Toxicol In Vitro 92(10):105663. DOI: 10.1016/j.tiv.2023.105663

Mas-Bargues C, Escrivá C, Dromant M, Borrás C, Viña J. 2021. Lipid peroxidation was measured by chromatographic determination of malondialdehyde. Human plasma reference values for health and disease. Arch Biochem Biophys 709. DOI:10.1016/j.abb.2021.108941

Meira CS, Soares JWC, dos Reis BPZC, Pacheco LV, Santos IP, Silva DKC, …, Soares MBP. 2022. Therapeutic applications of physalins: Powerful natural weapons. Front Pharmacol 13(4):1–14. DOI:10.3389/fphar.2022.864714

Melchart D, Hager S, Albrecht S, Dai J, Weidenhammer W, Teschke R. 2017. Herbal traditional chinese medicine and suspected liver injury: A prospective study. World J Hepatol 9(29):1141–1157. DOI:10.4254/wjh.v9.i29.1141

Moghadam MT, Dadfar R, Khorsandi L. 2021. Effects of ozone and melatonin on busulfan-induced testicular damage in mice. J Bras Reprod Assist 25(2):176–184. DOI:10.5935/1518-0557.20200081

Qin S, Wang J, Yuan H, He J, Deng Y. 2023. Liver function indicators and risk of hepatocellular carcinoma: A bidirectional Mendelian randomization study. Front Genet 14(1):1–7. DOI:10.3389/fgene.2023.1260352

Qin Y, Liu L, He Y, Wang C, Liang M, Chen X, …, Wang D. 2016. Testicular busulfan injection in mice to prepare recipients for spermatogonial stem cell transplantation is safe and nontoxic. PLoS One 11(2):1–15. DOI:10.1371/journal.pone.0148388

Silva-Santana G, Bax JC, Fernandes DCS, Bacellar DTL, Hooper C, Dias AASO, …, Mattos-Guaraldi AL. 2020. Clinical hematological and biochemical parameters in Swiss, BALB/c, C57BL/6, and B6D2F1 Mus musculus mice. Anim Model Exp Med 3(4):304–315. DOI:10.1002/ame2.12139

Singh S, Osna NA, Kharbanda KK. 2017. Treatment options for alcoholic and nonalcoholic fatty liver disease: A review. World J Gastroenterol 23(36):6549–6570. DOI:10.3748/wjg.v23.i36.6549

Teja PTHS, Arjana AAG, Setiasih NLE, Merdana IM. 2021. the impact of oral administration of minyak rajas on liver histopathology and aminotranspherase activities in male kampong chicken. Indones Med Veterinus 10(2):233–244. DOI:10.19087/imv.2021.10.2.233

van der Velden WJFM, de Weerd-de Jong EC, de Haan AFJ, Blijlevens NMA. 2018. Busulfan-dependent hepatotoxicity of anti-thymocyte globulin formulations during conditioning for hematopoietic stem cell transplantation. Biol Blood Marrow Transplant 24(2):410–412. DOI:10.1016/j.bbmt.2017.10.020

Wang L, Wu H, Yang F, Dong W. 2019. Protective effects of myricetin against cardiovascular diseases. J Nutr Sci Vitaminol 65(6):470–476. DOI:10.3177/jnsv.65.470

Wiraswati HL, Ekawardhani S, Rohmawaty E, Laelalugina A, Zuhrotun A, Hendriani R, …, Dewi S. 2024. Antioxidant, anti-inflammatory, and antifibrotic activities of ciplukan (*Physalis angulata* L) extract. J Inflamm research 17:6297–6306. DOI: 10.2147/JIR.S470318

Wu K, Huang R, Wu H, Liu Y, Yang C, Cao S, …, Wu C. 2016. Collagen-binding vascular endothelial growth factor attenuates CCl4-induced liver fibrosis in mice. Mol Med Rep 14(5):4680–4686. DOI:10.3892/mmr.2016.5826

Xiang D, Zou J, Zhu X, Chen X, Luo J, Kong L, Zhang H. 2020. Physalin D attenuates hepatic stellate cell activation and liver fibrosis by blocking TGF-β/Smad and YAP signaling. Phytomedicine 78(1):153294. DOI:10.1016/j.phymed.2020.153294

Zhao Y, Zhao S, Liu S, Ye W, Chen WD. 2025. Kupffer cells, limelight in liver regeneration. Int Immunopharmacol 146(12):113808. DOI:10.1016/j.intimp.2024.113808